Journal of Mines, Metals and Fuels, *73(4): 951-958; 2025. DOI: 10.18311/jmmf/2025/48309*

Print ISSN : 0022-2755

Journal of Mines, Metals and Fuels

**Contents available at:** *www.informaticsjournals.co.in/index.php/jmmf*

# Optimization Optical Properties of CuS/CdTe Quantum Dots Synthesised by a Facile Green Synthesis

**Ravindar Adla[1], Veera Swamy Maragani[1], Ramesh Suramoni[2], Mohan Babu Nandru[3], Madhuri Dumpala[1] and Madhukar Katakam[1]***

*[1]Department of Physics, University College of Science, Osmania University, Hyderabad - 500007, Telangana, India; mkatakam28@gmail.com*

*[2]Department of Physics, Guru Nanak Institute of Technology, Ibrahimpatnam, Hyderabad – 501506, Telangana, India*

*[3]Department of Physics, South Campus, Telangana University, Kamareddy - 503101 Telangana, India*

## Abstract

*The semiconducting Quantum Dots (QDs) exhibits distinctive optical and chemical properties, depending on their size, which makes them suitable for many applications, including optoelectronics devices. The CuS/CdTe quantum dots were synthesized using plant mediated green method, by varying CuS concentration. The green method for synthesizing QDs in an open-air environment, minimizing the requirement of regulated atmospheric conditions. These quantum dots synthesized were characterization using Fourier-Transform Infrared [FTIR], UV-Vis, and Photo-Luminescence (PL) spectroscopy methods. Observed vibrational modes of Cu–S and Cd–Te are 620 $cm^{-1}$, 1155 $cm^{-1}$, respectively in the FTIR spectra. The optical properties were derived from UV spectra, with the distinct absorption band at shorter wavelengths suggesting the confinement of electrons and holes, leading to excitonic attraction in the CuT0.5 sample. The optical band gap values for CuS, CuT0.5, CuT1, CuT3 were derived from their respective Tauc's plots. The estimated of band gap value of CuS is 3.6 eV, which is larger than the other compositions CuS/CdTe. The absorption spectra for each of these samples were acquired from 350 to 750 nm wavelengths at room temperature. The Photoluminescence emission characterized by symmetric peaks validates the initial excitonic transitions and serves as a distinctive photoluminescence feature of CdTe quantum dots. The PL peak clearly shows a red-shift from 540 nm to 620 nm with increasing concentration of CuS. The observed red shift in the photoluminescence emission peak, could be attributed to the size-dependent confinement effect present in the quantum dots. The larger quantum dots demonstrate a decreased energy gap resulting from diminished confinement of the carrier photons. These novel quantum dots synthesized through green methods showed excellent optical properties and suitable for energy conversion and storage applications.*

***Major Findings:** The CuS/CdTe quantum dots were successfully synthesized by varying CuS concentrations, using green methods. Optical band gap of CuS is higher than the composition of CuS/CdTe. Observed red-shift in the photoluminescence emission spectra with increasing concentration of CuS, due to the size-dependent confinement effect of the quantum dots.*

**Keywords:** Band Gap Energy, CuS/CdTe, Quantum Dots, Optical Properties, Photo-Luminescence

## 1.0 Introduction

Nanomaterials having the dimensions in the range of 1 to 10 nm, show distinctive size-dependent physiochemical properties, including semiconducting Quantum Dots (QDs) materials. The remarkable absorption of sunlight

*Author for correspondence

exhibits a significant peak shift associated with a wide absorption spectrum, alongside a narrow and symmetric emission peak of light. The capacity to precisely adjust the QD emission peak, nearly the entire visible region renders them an excellent alternative to traditional organic fluorophores[1,2]. The synthesis can be conducted under various environments to attain a light of maximum emission peak. This tunability, a more straightforward term, facilitates the development of QDs exhibiting diverse emission colors. The capacity to change these colors using combination environment presents a notable benefit, enabling precise control over the emission color, which is dictated by the photoluminescence maximum emission peak position. The stability and underlying mechanism of sensing are significantly influenced by the precise choice of emission wavelength[3]. In biosensing applications, the sensing exhibition and instrument of CdTe quantum dots are significantly influenced by the precise selection of their PL emission peak position[4]. In a similar vein, in chemo sensing applications, the quantum dots can be modified through a particle that is attached to a specific board usually. The interaction between the board usual and the QDs results in a modification of fluorescence of quantum dots[5]. Their remarkable optical properties, their application has expanded significantly in recent decades across various fields, including medical imaging, biosensing, and in solar cells, transistors, and LEDs[6]. The QDs consist of a CuS that may be enveloped by a CdTe, typically composed of essentials from IIB-VIB, IIIB-VB, and IVB-VIB groups of the periodic table[7].

The inorganic CuS play a crucial role in determining the optical properties of the nanoparticles, while the CdTe, made up, is essential for stabilizing the improving the quantum of emission yield. The size of quantum dots is less than the Bohr radius of the component materials, resulting in the manifestation of the quantum confinement emission effect. Which allows for the modulation of fluorescence emission, which is directly influenced by the particle size and the conformation of the quantum dots, including both the CuS and CdTe materials. A smaller diameter of the QD results in a higher energy value of its band gap, leading to a lower emission peak position of materials[8]. Often referred to as the reacted intensity of enhances the permanency of quantum dots, while enabling precise controller over the size distribution and morphology of the nanoparticles. They significantly enhance the intensity of peak emission by facilitating the development of a covalent bond between copper sulfate and in part corresponding $Cd^{2+}$ ionic radius on the surface of the quantum dots[9]. The CuS/CdTe quantum dots are widely utilized because of their diminutive size and the straightforward methods available for their acquisition through various direct green synthesis techniques[10].

Various methods can be employed to prepare these nanocrystals, either through top-down or through bottom-up methods. Currently, there is a growing interest in developing more environmentally friendly green methods for their synthesis[11]. The synthesis of nanomaterials via microwave dielectric heating, such as the CuS/CdTe QDs, in a examined the effect of different reactions of materials. The synthesized quantum dots exhibited a surface morphology, with dimensions ranging from 3 to 5 nm. The literature reveals the optimization of CuS/CdTe quantum dots synthesis, examining the impact of various parameters. Nonetheless, there is an absence of green procedures and size regulation, along with a lack of λ max of emission peak, which obscures the green process and renders them less appealing for optical properties, particularly in the materials, where size and light color are critical characteristics[12].

The application of experimental analysis facilitates the simultaneous examination of various bounds, leading to a decrease in costs related to synthesis procedures. Our analysis indicates that there is a lack of literature specifically aimed at the specific control of the maximum emission photoluminescence of CuS/CdTe quantum dots synthesized through the green method. as a substitute for traditional hydrothermal synthesis methods, it presents a significant non-classical energy source due to its capability for heating of the solution in a reduced timeframe. The optimization of synthesis was carried out through experimental design, focusing on specific factors of different materials and the combination of CuS and CdTe quantum dots[13-15]. The implementation of green method facilitated the synthesis of CuS/CdTe QDs exhibiting a range of wavelengths and colors, spanning from green to red, which correlate with varying sizes. The high stability of the as-synthesized CuS/CdTe QDs.

## 2.0 Material and Method

### 2.1 Materials

All the chemical of AR grade. The Chloroform ($CHCL_3$), Methanol ($CH_3OH$), Sodium sulphate ($Na_2SO_40$, Cadmium sulphate ($CdSO_4$) (99.5% m.w: 256.50), Copper sulphate ($CuSO_4$) (98.5% m.w: 159.609), deionized water, were acquired from SD Fine Chemicals Ltd., India. The Tellurium powder (Te) (m.w: 78.96) purchased from Sigma-Aldrich Pvt. Ltd., India. The *Moringa oleifera* leaves are collected from local gardens of Osmania University Campus, Hyderabad, Telangana state, India.

### 2.2 Preparation of Leaf Extract

Fresh *Moringa oleifera* (MO) leaves, abundantly available at the Osmania University campus garden, were collected and cleanly washed for several times. These leaves were air-drying in the shade for 5 hours and then finely cut and ground using a micro-grinding machine to make smaller pieces. About 20 g of these leaves were added with 100 mL of methanol. This was kept in an incubator/agitator at 70°C for 95 minutes. After cooling the solution, filtered using Whatman No. 1 filter paper, to get a clear extract.

### 2.3 Preparation of CuS and CdTe Quantum Dots

To synthesize CuS and CdTe quantum dots, a solution of 0.25 M $CuSO_4$ in 5 mL of distilled water was prepared and stirred for 20 minutes. This solution served as the precursor for subsequent synthesis steps. Different concentrations of 0.24 M, 0.57 M, and 1.28 M solutions were prepared. About 1:1 molar ratio of 10 mL of 0.24 M $CdSO_4$ and 0.57 M Tellurium (Te) powder was dissolved in 15 mL of distilled water and stirred for 40 minutes, producing a clear, soluble solutions. This was used as a precursor in the synthesis of CdTe nanoparticles. In the first phase, 15 mL of 0.24 M $CuSO_4$ was prepared and combined with 15 mL of CdTe solution (at concentrations of 0.24 M and 0.57 M) and 20 mL of Moringa oleifera leaf extract. In the second phase, 15 mL of 0.14 M $Na_2SO_4$ was added to the mixture and incubated under similar conditions for an additional 5 days. The resulting solution was centrifuged to isolate nanoparticles. The nanoparticles were then dried in a hot air oven at 90°C for 3 hours, producing a dry solid pellet for further characterization studies. The entire process is shown as Figure 1.

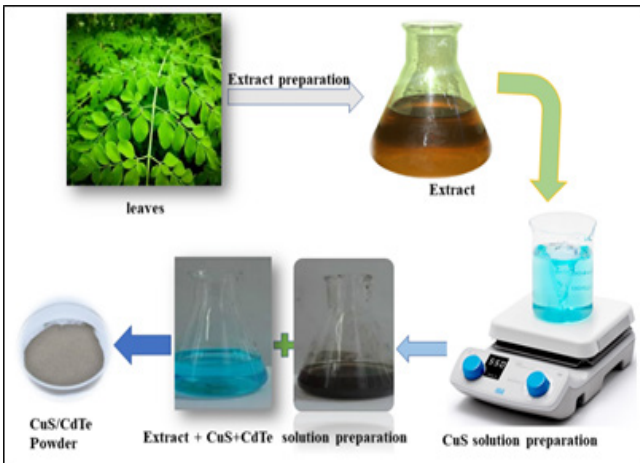



**Figure 1.** Synthesis of CuS/CdTe quantum dots using MO leaf extract.

## 3.0 Characterization Techniques

The synthesized CuS/CdTe QDs were analyzed using different spectroscopic methods. The distinct insights into the quantum dots, the UV-Visible spectroscopy was utilized to evaluate the optical properties in the range of wavelength 200 to 800 nm. The FTIR spectroscopy was applied to verify various interactions in CuS/CdTe based QDs. The Bruker Alpha FTIR spectrometer was employed to record the IR spectra. The CuS/CdTe QDs experienced characterization through absorbance measurements using the Thermo Scientific Evolution 201 and photoluminescence analysis with the Ocean Optics Spectrometer, USB4000-XR1-ES.

## 4.0 Experimental Analysis

### 4.1 FTIR Analysis of CuS/CdTe QDs

The FTIR analysis is a green method for identifying the characteristics of materials and provides insights into the impurities present in the deposits. The FTIR spectrum prominently features C-O and C-C stretching vibrations as shown in Figure 2. The peaks identified in this spectrum signify the stretching bending vibrations 511 $cm^{-1}$ linked to Cu-S bond vibrations and the symmetric stretching of Cu-S transpires around 568 $cm^{-1}$. The band peak at 1144

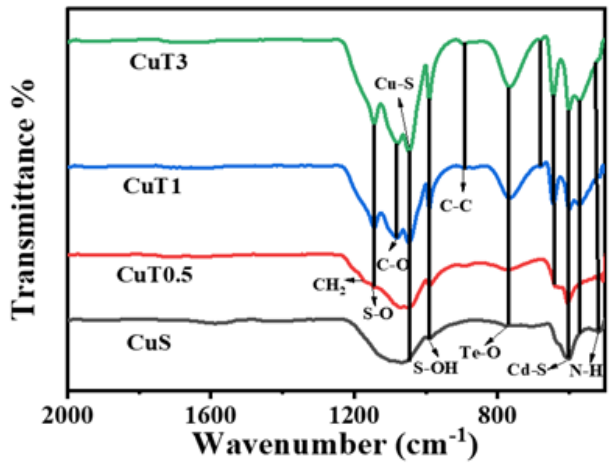



**Figure 2.** FTIR spectra of CuS/CdTe loaded with different CuS concentrations.

$cm^{-1}$ is the vibrational mode of Cd-Te bond, may also occur often in proximity to the detection of peaks within this, confirms the formation of CuS and CdTe phases[15]. The presence of 1047 $cm^{-1}$ mode associated with lattice vibrations may arise in CuS systems. Signal identified in this context suggest the presence of secondary phases corresponding to such as CdO and CuO. Peak at 992 $cm^{-1}$ indicate the presence of sulfate (S-OH) bond, resulting from the oxidation of CuS, examine this area for indications of pollution and oxidation effects. All vibration peak positions are summarized in Table 1. The peak detected at 772 $cm^{-1}$ is indicate the presence of oxidation effect. The Weak peak position of band vibration to Te-O to be detected in 1202 $cm^{-1}$. The prominent peak at 789 $cm^{-1}$ often increase from water absorption the existence of hydroxyl (-OH) groups on the surface. The peak detected at 1052 $cm^{-1}$ indicates moisture content and affects the stability of the CuS/CdTe surface alterations and specific dopants[16], significant peak is expected in this scenario for a pure CuS. The detection of peaks at 652 $cm^{-1}$ confirms the formation of Cu-S and Cd-Te bond. The vibrational band peak shift at 892 $cm^{-1}$ indicates interfacial interactions corresponding to CuS/CdTe the existence of oxidation associated with C-C bonds. The extent can be evaluated for hydroxyl contamination. The variations in the primary peaks of Cu-S indicate the existence of lattice stress, defects, and non-stoichiometry CuS/CdTe quantum dots.

## 4.2 Photoluminescence of CuS/CdTe QDs

The CuS/CdTe QDs underwent characterization through absorbance measurements using the Thermo Scientific Evolution 201 and photoluminescence analysis with the

**Table 1.** The FTIR peak positions of CuS, CuT0.5, CuT1, CuT3

| Vibrational modes | CuS | CuT0.5 | CuT1 | CuT3 |
|---|---|---|---|---|
| N-H stretching vibration | 511 | 517 | 568 | 567 |
| Cd-S stretching vibration | 652 | 638 | 681 | 678 |
| Te-O stretching vibration | 772 | 778 | 769 | 768 |
| C-C stretching vibration | - | 892 | 896 | - |
| S-OH stretching vibration | 992 | 990 | 992 | 988 |
| Cu-S stretching | - | 1047 | 1045 | 1044 |
| C–O Stretching vibration | 1052 | - | 1088 | 1085 |
| S-O stretching vibration | - | 1144 | 1139 | 1141 |
| CH2 asymmetric Stretching vibrations | - | 1202 | 1203 | - |

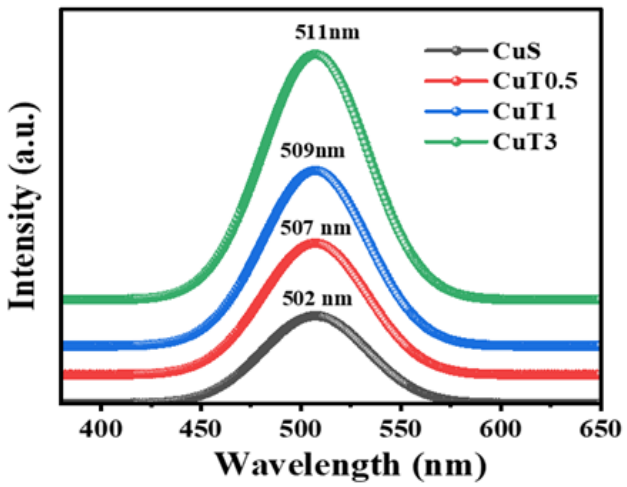



**Figure 3.** Photoluminescence spectra of CuS/CdTe QDs loaded with different concentrations of CuS.

Ocean Optics Modular Spectrometer, USB4000-XR1-ES. The relationship between the size of the quantum dots and the refluxing time was determined through numerical calculations based on the measured wavelengths of PL peaks. The room temperature photoluminescence spectra of the CuS/CdTe quantum dots, synthesized with varying refluxing durations at 20-minute intervals, were measured using a 450 nm excitation wavelength and are presented in Figure 3. To facilitate comparative analysis, the PL intensity of all samples has been normalized. The absorption spectra for each of these samples was acquired from 350 nm to 750 nm wavelengths at room temperature, as illustrated. It is observed in the absorption spectrum, that the CuS, PL emission peak pertaining to CuS/CdTe quantum dots, show a strong correlation with CuT3. These findings are aligned closely with literature[17]. The data presented indicates that the PL emission peaks exhibit notable strength and a commendable level of symmetry across all systems. The pronounced room-temperature photoluminescence emission characterized by symmetric peaks validates the initial excitonic transitions and serves as a distinctive photoluminescence feature of CuS/CdTe quantum dots[18,19]. Furthermore, the symmetric Gaussian characteristics, along with, suggest that the size distribution of the suspended QDs in the solutions is relatively narrow. The PL peak clearly shows the emission max, red-shift from 540 nm to 620 nm with increasing refluxing time. The clear red-shift associated with the sharp onset of absorption as refluxing time increases is also quite apparent. The observed red shift in the absorption onset and photoluminescence emission peak as refluxing time increases, can be attributed to the size-dependent confinement effect of the quantum dots. During the refluxing process at the boiling temperature of the solution mixture, the particles of CdTe increase in size. Consequently, the solution exhibits larger quantum dots of CuS/CdTe as the refluxing process persists. The larger quantum dots demonstrate a decreased energy gap resulting from diminished confinement of the carriers, leading to a red-shift in the photoluminescence absorption spectra[20].

**Table 2.** Photoluminescence [PL] λ max of samples CuS, CuT0.5, CuT1, CuT3

| Sl. No | Samples | Em [λmax] |
|---|---|---|
| 1 | CuS | 502 |
| 2 | CuT0.5 | 507 |
| 3 | CuT1 | 509 |
| 4 | CuT3 | 511 |

## 4.3 UV-Visible and Bandgap energy of CuS/CdTe based QDs

The UV-Visible absorbance peaks positions. The extended duration of refluxing is likely responsible for

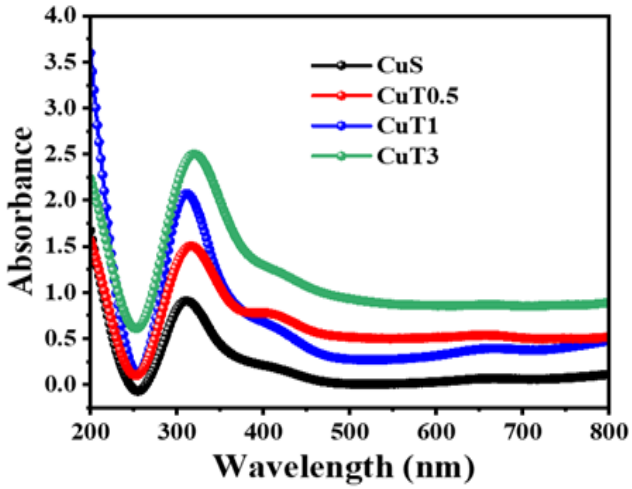



**Figure 4.** UV-visible absorbance spectra of CuS, CuT0.5, CuT1, CuT3 samples.

**Table 3.** UV-visible absorbance spectrum of CuS/CdTe of samples

| Sl. No | Samples | Wavelength [nm] | Absorbance |
|---|---|---|---|
| 1 | CuS | 310 | 1.52 |
| 2 | CuT0.5 | 315 | 1.45 |
| 3 | CuT1 | 310 | 2.08 |
| 4 | CuT3 | 319 | 2.26 |

the observed phenomenon. Figure 4, which presents the UV-Vis absorbance spectra. This process may contribute to resulting various of samples[21]. The absorbance excitonic peaks positions from the Table 3. was observed at approximately 490 nm for sample CuT0.5, and it shifts to around 521 nm as the refluxing concentration increases. The observed high shift of the absorbance peak with increasing various suggests a growth in the size of CuS/CdTe quantum dots, attributed to quantum confinement[22]. The intensity of the absorbance peak for the quantum dots in the sample shows

This occurs because there is a greater quantity of CdTe monomers present with increased refluxing durations. The CuS/CdTe quantum dots, even after extending the optical band gaps energy (Eg) of the quantum dots are valued utilizing Tauc's Equation (1)[23].

$$(\alpha h\vartheta)^2 = A(h\vartheta - Eg) \quad (1)$$

In this context, 'A' represents the Tauc's plot, 'hυ' denotes the photon energy, 'α' signifies the absorption coefficient, and 'm' indicates the evolution probability. In materials exhibiting a direct band gap, the value of 'm' is ½ for permitted transitions[24]. The plots of ' between 'hυ' for the systems are illustrated in Figure 5. The estimated optical band gap values for the samples CuS, CuT0.5, CuT1, CuT3 derived from their respective Tauc's plots, are approximately 3.6, 3.5, 3.4, and 3.2 eV, respectively, as detailed in the Table 4. The calculated values of band gaps appear to be significantly larger when compared to the bulk CdTe band gap energy[25-26].

**Table 4.** Bandgap energy of CuS, CuT0.5, CuT1, CuT3

| Sl.No | Samples | Eg (eV) |
|---|---|---|
| 1 | CuS | 3.6 |
| 2 | CuT0.5 | 3.5 |
| 3 | CuT1 | 3.4 |
| 4 | CuT3 | 3.2 |

## 5.0 Conclusion

In conclusion, we utilised an environmentally friendly method to synthesise stabilised CuS/CdTe QDs in an aqueous phase, ensuring precise control over the growth of CuS. The luminescence quantum yield of CuS/CdTe quantum dots were improved through surface passivation using CuS of optimal. The vibrational modes of Cu-S and Cd-Te appeared at 600cm$^{-1}$, 1150 cm$^{-1}$, respectively. The optical properties were derived from UV–Vis spectra, with the distinct absorption band at shorter wavelength, suggesting the confinement of electrons and holes, leading to excitonic and Coulombic attraction in the two samples. The optical band gap was determined and analysed in relation to the bulk materials. The luminescence of the CuS/CdTe QDs arises not only from the recombination of an electron from CuS with a hole from CdTe but also from the recombination of an electron and a hole that are confined within CdTe. There was a notable increase in absorption within the visible region, showing a greater reliance for CdTe. While different wavelength provides bandgap energies 3.6 eV and 3.2 eV (associated with a spin-orbit), a red shift is observed in $E_g$ 3.4 eV. The photoluminescence decay and quantum yield of CuS/CdTe quantum dots were associated with the surface passivation of CuS and the surface traps present in CdTe. The processes collaboratively influenced the PL decay behaviour. The extension of the radiative lifetime was validated in CuS/CdTe QDs with the rise of CuS, signifying the progression of CuS/CdTe QDs. Green synthesized CuS/CdTe QDs demonstrated excellent optical and electronic properties makes them suitable for several applications in optical electronics, environmental and energy conversion and storage.

## 6.0 References


1. Ajroud M, Abdella FIA, Alanazi TYA, Helaoui M, Boudriga S. Exploring the probing capacities of MSA capped CdTe semiconductor quantum dots as optical chemosensors via analytical and isotherm modeling for selective $Hg^{2+}$ detection. Appl Water Sci. 2024; 14(2):15. https://doi.org/10.1007/s13201-023-02078-y
2. Nhan NT, Duc VA, Dung MX, Bac HQ. Effects of Zn(II) on the optical properties of CdTe quantum dots and their photoluminescence response to lead ion. VNU J Sci Nat Sci Technol. 2022. https://doi.org/10.25073/2588-1140/vnunst.5286
3. Kadim MA. Applications of cadmium telluride (CdTe) in nanotechnology. In: Nanomaterials - Toxicity, Human Health, and Environment. Intech Open; 2020. https://doi.org/10.5772/intechopen.85506
4. Rezanejade Bardajee G, Hooshyar Z. CdTe quantum dots embedded in multidentate biopolymer based on Salep: Characterization and optical properties. J Chem. 2013; 2013(1). https://doi.org/10.1155/2013/202061
5. Patan Alper FM. Aqueous synthesis of CdTe quantum dots and optical characterization under high voltage. Acta Phys Pol A. 2023; 143(3):221-7. https://doi.org/10.12693/APhysPolA.143.221
6. Čapek RK, Moreels I, Lambert K, De Muynck D, Zhao Q, Van Tomme A, *et al*. Optical properties of zincblende cadmium selenide quantum dots. J Phys Chem C. 2010; 114(14):6371-6. https://doi.org/10.1021/jp1001989
7. Lee T, Enomoto K, Ohshiro K, Inoue D, Kikitsu T, Hyeon-Deuk K, *et al*. Controlling the dimension of the quantum resonance in CdTe quantum dot superlattices fabricated via layer-by-layer assembly. Nat Commun. 2020; 11(1):5471. https://doi.org/10.1038/s41467-020-19337-0
8. Shen M, Jia W, You Y, Hu Y, Li F, Tian S, *et al*. Luminescent properties of CdTe quantum dots synthesized using 3-mercaptopropionic acid reduction of tellurium dioxide directly. Nanoscale Res Lett. 2013; 8(1):253. https://doi.org/10.1186/1556-276X-8-253
9. Ramalingam G, Ragupathi C, Rangasamy B, Colak I, Vetrivelan V, Poudineh N, *et al*. [Retracted] Structural and optical properties of CdSe/CdTe core-shell quantum dots. J Nanomater. 2022; 2022(1). https://doi.org/10.1155/2022/6316716
10. Li L, Yang S, Jing W, Jiang Z, Han F. Enhanced photocurrent gain by CdTe quantum dot modified ZnO nanowire. Sens Actuators A Phys. 2015; 232:292-8. https://doi.org/10.1016/j.sna.2015.06.020
11. Kassem M, Kassem H, Bychkov E. Macroscopic and electric properties in the CdTe-AgI-$As_2Se_3$ system. Mater Res Bull. 2018; 107:264-70. https://doi.org/10.1016/j.materresbull.2018.07.035
12. Kiprotich S, Dejene BF, Onani MO. Structural, optical, and luminescence properties of CdTe quantum dots: Investigation on the effect of capping ligand ratio. Mater Res Express. 2018; 5(6):065028. https://doi.org/10.1088/2053-1591/aac938
13. da Costa PFGM, Merízio LG, Wolff N, Terraschke H, de Camargo ASS. Real-time monitoring of CdTe quantum dots growth in aqueous solution. Sci Rep. 2024; 14(1):7884. https://doi.org/10.1038/s41598-024-57810-8
14. Borah DJ, Saikia D, Das A, Saikia PK, Mostako ATT. An investigation on the structural and optical properties of mercaptosuccinic acid capped cadmium telluride quantum dots. Discov Mater. 2023; 3(1):4. https://doi.org/10.1007/s43939-023-00041-x
15. Gharibshahi E. Simulation, synthesis, and optical properties of cadmium telluride (CdTe) semiconductor nanoparticles. Solid State Commun. 2020; 320:114009. https://doi.org/10.1016/j.ssc.2020.114009
16. Hernández-Granados A, Escorcia-García J, Peréz-Martínez D, García-Cerrillo J, Menchaca-Campos C, Hu H. $Sb_2(S_xSe_{1-x})_3$ sensitized solar cells prepared by solution deposition methods. Mater Sci Semicond Process. 2016; 56:222-7. https://doi.org/10.1016/j.mssp.2016.08.022
17. Li H, Lu W, Song B, Zhou J, Zhao G, Han G. The design of $Mn^{2+}$ and $Co^{2+}$ co-doped CdTe quantum dot sensitized solar cells with much higher efficiency. RSC Adv. 2020; 10(59):35701-8. https://doi.org/10.1039/D0RA06381A
18. Suria Moorthy P, Zhang X, Hao G, Joly AG, Singh S, Hossu M, *et al*. Folic acid-CdTe quantum dot conjugates and their applications for cancer cell targeting. Cancer Nanotechnol. 2010; 1(1-6):19-28. https://doi.org/10.1007/s12645-010-0003-3
19. Tomar S, Gupta S, Priyam A, Bhushan B, Singh A, Dwivedi UK, *et al*. Temporal evolution of optical absorption and emission spectra of thiol capped CdTe quantum dots. Appl Phys A. 2022; 128(10):944. https://doi.org/10.1007/s00339-022-06087-7
20. Salih Ajaj C, Sadiq D. Mulberry juice-derived carbon quantum dots as a $Cu^{2+}$ ion sensor: Investigating the influence of fruit ripeness on the optical properties. Nanomater Nanotechnol. 2023; 2023:1-11. https://doi.org/10.1155/2023/9980479

21. Yao J, Yang M, Duan Y. Highly fluorescent CdTe nanocrystals: Synthesis, characterization, property, mechanism, and application as a sensor for biomolecule analysis. J Mater Res. 2014; 29(5):633-40. https://doi.org/10.1557/jmr.2014.25
22. Li G, Fei X, Liu H, Gao J, Nie J, Wang Y, *et al*. Fluorescence and optical activity of chiral CdTe quantum dots in their interaction with amino acids. ACS Nano. 2020; 14(4):4196-205. https://doi.org/10.1021/acsnano.9b09101
23. Chen Y, Wu Y, Weng B, Wang B, Li C. Facile synthesis of nitrogen and sulfur co-doped carbon dots and application for Fe(III) ions detection and cell imaging. Sens Actuators B Chem. 2016; 223:689-96. https://doi.org/10.1016/j.snb.2015.09.081
24. da Rosa L, Aversa I, Raphael E, Polo A, Duarte A, Schiavon M, *et al*. Improving photoluminescence quantum yield of CdTe quantum dots using a binary solvent (water + glycerin) in the one-pot approach synthesis. J Braz Chem Soc. 2021. https://doi.org/10.21577/0103-5053.20200237
25. Wu H, Zhang W, Li K, Liu C. Optical properties of CdTe quantum dots in silicate glasses containing CaO. Opt Mater (Amst). 2024; 148:114897. https://doi.org/10.1016/j.optmat.2024.114897
26. Olawale F, Oladimeji O, Ariatti M, Singh M. Emerging roles of green-synthesized chalcogen and chalcogenide nanoparticles in cancer theranostics. J Nanotechnol. 2022; 2022:1-18. https://doi.org/10.1155/2022/6176610